Journal of Materials and Electronic Devices 2 (2023) 21-28



DFT Based Quantum Chemical Descriptors of Favipiravir Forms

^a·Hakan Sezgin Sayiner, ^bSerap. Sentürk Dalgıc, ^cFatma. Kandemirli*

^aInfectious Diseases, Medicine Department, Adiyaman University, Adiyaman, Turkey
^bAtomic and Molecular Physics, Physics Department, Faculty of Science, Trakya University, Edirne, Turkey
^cBiomedical Engineering Department, Faculty of Engineering and Architecture, Kastamonu University, Kastamonu, Turkey

This research has focused on the chemical reactivity behavior of favipiravir forms and the transition states of forms. These compounds are potential drugs for the Ebola virus and have shown their effectiveness for COVID-19. Geometry optimizations have been conducted by using the DFT method with the B3LYP/6-311G(d,p) method in the gas phase and 4 different solvent environments. The Polarized Continuum Model has been used to evaluate the solvent effect on chemical stability and their related properties. Dipole moment, polarizability, and molecular first-order hyperpolarizability of the favipiravir forms were computed for the gas and solvent phase. Also, thermodynamic properties such as heat capacity, entropy, and enthalpy of the A3 form of favipiravir at different temperatures were calculated in the gas phase.

Keywords: Bioceramics, Favipiravir, Covid-19, B3LYP, solvent effect, Tautomer.

Submission Date: 17 March 2023 Acceptance Date: 15 June 2023

*Corresponding author: fkandemirli@yahoo.com

1. Introduction

T-705 (favipiravir), a fluorinated pyrazine carboxamide was initially developed against influenza viruses [1]. T-705 (Favipiravir) is an antiviral pyrazine carboxamide-based, inhibitor of the influenza viruses with an EC90 of 1.3 to 7.7 uM (influenza A, H5N1). T-705 exhibits activity against type B and C viruses with EC90s of 0.25-0.57 uM and 0.19-0.36 uM, respectively [2]. Favipiravir acts as a purine analog that selectively inhibits viral RdRps [3]. In addition to its potent anti-influenza activity, favipiravir has shown activity against a wide range of other RNA viruses, including enteroviruses, bunyaviruses, filoviruses, norovirus, arenaviruses, flaviviruses rhabdoviruses, and alphaviruses [4-6]. They reported that favipiravir had potent antiviral activity against henipaviruses and showed that In vitro, favipiravir inhibited Nipah and Hendra virus replication and transcription at micromolar concentrations. In the Syrian hamster model, either twice-daily oral or once-daily subcutaneous administration of favipiravir for 14 days fully protected animals challenged with a lethal dose of Nipah virüs [7]. In February 2020, the drug

favipiravir began to be studied in China for its experimental treatment in COVID-19 (new coronavirus) disease, which appeared in China [8]. Parlak et al, [9] investigated the adsorption between favipiravir and undoped or silicondoped C60 fullerenes to assess their possible usage as drug delivery vehicles and also they studied the possible interaction mechanism of C20 and Si-doped C20 fullerenes with favipiravir molecule [10]. They reported a structural analysis of favipiravir performed by exploring tautomers formations. They reported that four tautomers could be possible for favipiravir and their stability could be different regarding the values of total energy and also reported that the results indicated that the structure given in Fig 1. was the most stable structure and the next one is F1 by 5 kcal/mol difference in the stability level [11].

Fig. 1. The structures of favipiravir

In very recent studies, favipiravir has been studied for experimental treatments of COVID-19, where it is recommended as an effective drug recently [12]. Previous studies have shown that quantum chemical calculations can very well evaluate molecular properties [13-16]. Over the past two decades, there has been a great deal of interest in studying the tautomerism of heterocyclic compounds to ensure that the effect of tautomerism on the chemical and biological properties of molecules can be determined. These structures and tautomers can occur if the energy required for tautomer formation is provided by other sources, such as intermolecular interactions and binding, and may be important in recognizing such structures before exploring their activity in the biological environment [10]. This study aims to investigate two different structures (A and B) and three tautomers of structure A and two tautomers of structure B and transition states between the tautomers and conformers A and B in different environments as a quantum chemical. Besides, the temperature addiction of the thermodynamic parameters such as heat capacity (Cv), entropy (S), zero-point energy, and heat capacity at constant pressure was calculated at B3LYP /6-311G(d,p) level in the gas phase for A3 form.

2. Materials and Method

Gaussian 09 program [17] was used for all DFT calculations. Possible structures (Figure 2) in the gas phase and different media have been analyzed by performing density functional theory (DFT) calculations at the B3LYP/6-311G(d,p) theoretical level. computations based on the same geometry optimization method were used to confirm the nature of the stationary points. Frequency calculations characterized all stationary points. The reaction pathway was determined by following the IRC procedure [18,19]. In addition, the effects of four solvents, ethanol, DMF, DMSO and water were studied through the self-consistent reaction-field (SCRF) method based one conductor-like polarisable continuum model (CPCM), which is often considered one of the most successful solvation models [20]. The Polarizable continuity model (PCM) proposed by Born, Kirkwood and Onsager is an extension of the solvent reaction field models presented for charge distributions in space. PCM uses a more realistic shape of the void, simulates the dielectric response with separate charges on the void surface, and contains nonpolar additives to the solution [21]. The electronic energies, NLO properties, the energy of the highest occupied molecular orbital (E_{HOMO}), and the lowest unoccupied molecular orbital (E_{LUMO}) of the energy were computed. Also, some parameters related to HOMO and LUMO energies such as chemical hardness (h), chemical softness (S), electronegativity (χ), chemical potential (μ) and electrophilicity index (w) were computed. Nonlinear optical (NLO) properties such as dipole moment (u), mean polarizability (atotal), the anisotropy of the polarizability $(\Delta \alpha)$ and first hyperpolarizability (β) were computed with the B3LYP/6-311G(d,p) theoretical level.

3. Results and Discussion

Two different structures were considered (A and B). The features of three tautomers of structure A and two tautomers of structure B were examined. The transition states between the tautomers of structure A in gas and solvent phases were examined, and also the transition states of structure A and B were examined. The optimized possible molecular conformations of favipiravir numbering of the atoms, and its transition states forms with the sum of electronic and zero-point Energies calculated using B3LYP/6311 G(d,p) theoretical method in the gas phase were given in Fig. 2. No imaginary frequencies were found in the calculated vibrational spectra of the stable A1, A2, A3, B1, B2 form of favipiravir while a single imaginary stretching frequency was found for each Transition State (TS). The value of imaginary frequencies are -1893 cm⁻¹ for TS1, -515 cm⁻¹ for TS2, -1903 cm⁻¹ for TS3, in gas phase. The energies for the A1, A2, A3, B1, and B2 form of favipiravir and transition between A1 with A2, A2 with A3, and A3 with B1 are summarized in Table 1 for different media. The energies are sensitive to the gas phase and solvent used. On the other hand, transition states are characterized by higher energies compared to the other form. It is clear that the calculated values of the energies depend on the solvent media used. Accordingly, the energy is -381253 kcal/mol for A1 form, -381241 kcal/mol for A2 form and -381239 kcal/mol for A3 form. A1, A2 and A3 form are tautomer form each other. A1 is more stable than the others. A3 and B1 are different conformers of favipiravir molecule. B1 conformer is stable than A3 conformer however is less stable than A1 and A2 tautomer forms in gas phase and different media (Table 1). The order of stability of A1, A2, A3 tautomers studied in the gas phase and solvent media is A1 > A2 > A3.

Table 1 The energies for the A1, A2, A3, B1, and B2 form of favipiravir and transition between A1 with A2, A2 with A3, and A3 with B1 (Kcal/mol)

Form	gas	ethanol	DMF	DMSO	water
A1	-381253	-381260	-381260	-381260	-381260
TS2	-381241	-381249	-381249	-381250	-381250
A2	-381244	-381253	-381253	-381253	-381253
TS1	-381231	-381239	-381240	-381218	-381241
A3	-381239	-381253	-381253	-381253	-381253
B1	-381242	-381255	-381255	-381256	-381256
B2	-381242	-381252	-381252	-381253	-381253
Act1	12.27	10.76	10.74	10.72	10.71
Act2	13.35	14.03	12.74	34.80	12.72
Act3	2.47	2.57	2.59	2.75	2.9
ΔΕ1	8.59	7.01	6.99	6.97	6.96
$\Delta E2$	5.18	0.17	0.07	0.03	-0.04
ΔΕ3	13.77	7.18	7.05	7.00	6.92
$\Delta E4$	0.15	2.93	2.98	3.00	3.03

HOMO, LUMO ESP of A1, A2, A3, B1, B2 form and transition states were given in Fig. 2. HOMO is the outermost orbit filled with electrons; it can be thought of as a valance band as it is represented by the ionization potential of a molecule and acts as an electron donor. LUMO, on the other hand, represents the innermost orbital that is not filled by electrons and is directly related to electron affinity and it acts as an electron acceptor. The main orbitals involved in the chemical reaction are the highest-occupied molecular orbital (HOMO) and the lowest-occupied molecular orbital (LUMO) since they act as electron acceptors [22].

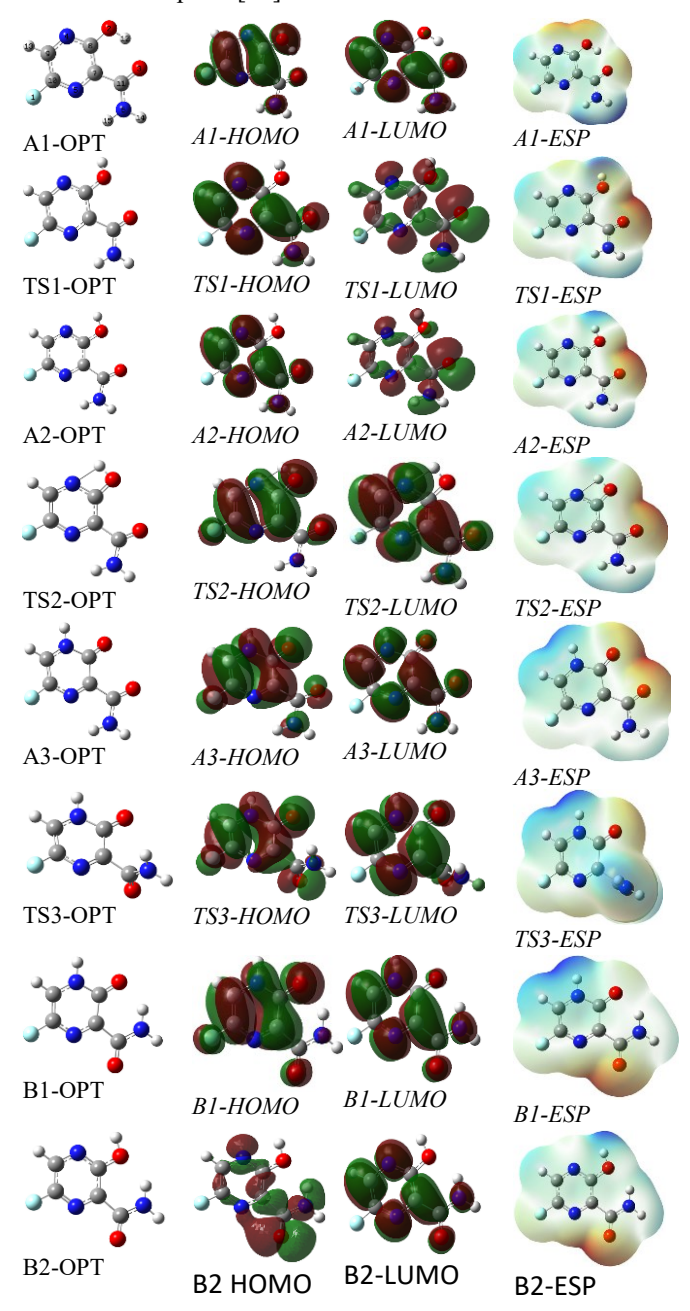


Fig. 2. Optimisation form, HOMO, LUMO ESP of A1, A2, A3, B1, B2 forms and transition states in different media

MEP map of the molecule is calculated in optimized geometries in estimating reactive regions for electrophilic and nucleophilic attack. In most MEPs, the maximum

negative region is indicated in red for electrophilic attack indications and the maximum positive region in blue for nucleophilic attack symptoms. In terms of colour grading, it shows molecular size, shape, positive, negative and neutral electrostatic potential regions simultaneously and MEP is very useful in the investigation of molecular structure with its physicochemical property relationship. The highest occupied molecular orbital (HOMO) and the lowest empty molecular orbital (LUMO) are called boundary orbitals, and these orbitals are key parameters in determining molecular properties and molecular electrical transport properties, the eigenvalues of HOMO (transmitter) and LUMO (receiver). Moreover, the energy difference between them determines the chemical activity of molecules. The Frontier molecular orbital energies have been calculated with B3LYP/6-311G (d,p) level. Results obtained from solvent (ethanol, DMF, DMSO and water) and gas-phase for of A1, A2, A3, B1, B2 form and transition states are listed in Table-2 with the parameters obtained from frontier molecular orbital.

Band gap Eg, electronegativity (χ), global hardness (η), chemical potential (μ), global electrophilic index (ω), spherical softness (S), Nucleofugality ΔEn and electrofugality ΔEe and electronic charge ($\Delta Nmax$) can be calculated using the following equations [23-25].

E_g =
$$E_{LUMO} - E_{HOMO}$$
 , $\eta \simeq -\left(\frac{E_{HOMO} - E_{LUMO}}{2}\right)$, $\mu = -\chi \simeq \left(\frac{E_{HOMO} + E_{LUMO}}{2}\right)$, $S = \frac{1}{2\eta}$, $\Delta E_n = -A + \omega = \frac{(\mu + \eta)^2}{2\eta}$, $\Delta E_e = I + \omega = \frac{(\mu - \eta)^2}{2\eta}$, $\Delta N_{max} = -\mu/\eta$

where ionization potential, I=-EHOMO and electron affinity, A=-ELUMO. The electrophilic index, chemical hardness, the chemical potential is a global reactivity index. ΔNmax refers to the maximum charge transfer to the electrophile. ΔNmax was evaluated as showing the ability of the system to obtain additional electronic charge from the medium that defines the charge capacity of the molecule. This index measures energy stabilization when the system receives an additional electronic charge (ΔNmax) from the environment. With the electronic chemical potential of the molecule, the direction of charge transfer is completely determined. Since an electrophile is a chemical type that can accept electrons from the environment, after accepting the electronic charge, its energy should decrease and the electronic chemical potential should be negative [26-29]. The global hardness index has changed as A3 < B1 < A1 < A2 < B2 for gas phase and studied solvent phase. It seems the structure A3 has the less hardness index and more reactive than the others. Table 2 represents the solvent effect of the ΔNmax for A1, TS1, A2, TS2, A3, TS2, B1, and B2 in different solvents. The max charge transfers index (ΔNmax) of A1, T1, A2, A3, TS3, B1 decreases as follow: gas > ethanol > DMF > DMSO > water. Δ Nmax of favipiravir forms increases in following order: B2 < A2 < A1 < B1 < A3 in gas phase, however in solvent phese (ethanol, DMF, DMSO, water) increase in following order:

Table 2. The theoretical E_{HOMO} , E_{LUMO} , ΔE , η , S, of favipiravir forms calculated by B3LYP/6-311 G(d,p) in gas phase and different solvents

S E_{HOMO} E_g E_{LUMO} gas -7.111 -2.567 4.544 2.272 0.220 et -7.081 -2.492 4.590 2.295 0.218 DMF-7.081 -2.491 4.590 2.295 0.218 **DMSO** -7.081 -2.490 4.591 2.295 0.218 water -7.081 -2.490 4.591 2.296 0.218 gas -7.095 -2.406 4.689 2.344 0.213 et -7.224 -2.374 4.850 2.425 0.206 DMF-7.226 -2.374 4.852 2.426 0.206 DMSO-7.227 -2.373 4.853 2.427 0.206 water -7.228 -2.373 4.855 2.428 0.206 gas -7.089 2.312 -2.465 4.624 0.216 et 4.745 -7.151 -2.406 2.373 0.211 DMF-7.150 -2.405 4.745 2.373 0.211 **DMSO** -7.150 -2.404 4.745 2.373 0.211 water -7.149 -2.404 4.745 2.373 0.211 gas -7.185 -2.541 4.645 2.322 0.215 ethanol -6.599 3.709 -2.890 1.855 0.270 DMF2.357 -7.138 -2.424 4.714 0.212 **DMSO** -6.872 -2.712 4.160 2.080 0.240 water -7.137 -2.422 4.715 2.358 0.212 gas -6.767 -2.857 3.910 1.955 0.256 et 3.901 1.951 -6.657 -2.756 0.256 DMF-6.655 -2.754 3.901 1.951 0.256 **DMSO** -6.655 -2.753 3.902 1.951 0.256 water -6.654 -2.752 3.902 1.951 0.256 gas -6.651 -2.480 4.171 2.086 0.240 ethanol -2.395 2.094 -6.582 4.187 0.239 DMF-6.580 -2.391 4.189 2.095 0.239 **DMSO** -6.579 -2.388 4.192 2.096 0.239 water -6.578 -2.387 4.191 2.096 0.239 gas -6.965 -2.896 4.069 2.034 0.246 et -6.790 -2.760 4.030 2.015 0.248 DMF-6.787 -2.758 2.014 4.029 0.248 **DMSO** -6.785 -2.757 4.028 2.014 0.248 water -6.784 -2.756 4.0282.014 0.248gas -7.158 -2.4204.738 2.369 0.211 et -7.248 -2.372 4.876 2.438 0.205DMF-7.245 -2.372 4.874 2.437 0.205 **DMSO** -7.244-2.371 4.873 2.436 0.205 water -7.243 2.436 -2.371 4.872 0.205 Et: ethanol

Table 3. The theoretical χ , μ , ω), ΔEn , ΔEe , $\Delta Nmax$, of favipiravir forms calculated by B3LYP/6-311 G(d,p) in gas phase and different solvents

		χ	μ	ω	∆En	∆Ee,	ΔN_{max}
	gas	4.839	-4.839	5.153	1.450	11.13	2.13
	et	4.787	-4.787	4.992	1.353	10.93	2.09
	DMF	4.786	-4.786	4.990	1.351	10.92	2.09
	DMSO	4.786	-4.786	4.989	1.351	10.92	2.09
	water	4.785	-4.785	4.987	1.350	10.92	2.08
	gas	4.751	-4.751	4.813	1.235	10.74	2.03
A2 TSI	et	4.799	-4.799	4.749	1.162	10.76	1.98
	DMF	4.800	-4.800	4.748	1.161	10.76	1.98
	DMSO	4.800	-4.800	4.747	1.161	10.76	1.98
	water	4.801	-4.801	4.746	1.160	10.76	1.98
	gas	4.777	-4.777	4.935	1.314	10.87	2.07
	et	4.778	-4.778	4.812	1.220	10.78	2.01
	DMF	4.778	-4.778	4.810	1.219	10.77	2.01
	DMSO	4.777	-4.777	4.809	1.218	10.77	2.01
	water	4.777	-4.777	4.808	1.218	10.77	2.01
	gas	4.863	-4.863	5.092	1.390	11.12	2.09
	et	4.744	-4.744	6.069	2.252	11.74	2.56
TS2	DMF	4.781	-4.781	4.848	1.246	10.81	2.03
, ,	DMSO	4.792	-4.792	5.520	1.768	11.35	2.30
	water	4.779	-4.779	4.845	1.244	10.80	2.03
43	gas	4.812	-4.812	5.921	2.087	11.71	2.46
	et	4.707	-4.707	5.678	1.947	11.36	2.41
	DMF	4.705	-4.705	5.674	1.944	11.35	2.41
	DMSO	4.704	-4.704	5.672	1.943	11.35	2.41
	water	4.703	-4.703	5.669	1.941	11.35	2.41
	gas	4.565	-4.565	4.997	1.474	10.61	2.19
	et	4.488	-4.488	4.811	1.369	10.35	2.14
TS3	DMF	4.485	-4.485	4.803	1.364	10.34	2.14
	DMSO	4.484	-4.484	4.795	1.360	10.33	2.14
	water	4.483	-4.483	4.794	1.359	10.33	2.14
	gas	4.931	-4.931	5.975	2.061	11.92	2.42
	et	4.775	-4.775	5.657	1.890	11.44	2.37
BI	DMF	4.772	-4.772	5.653	1.888	11.43	2.37
	DMSO	4.771	-4.771	5.651	1.887	11.43	2.37
	water	4.770	-4.770	5.648	1.885	11.43	2.37
B2	gas	4.789	-4.789	4.840	1.236	10.81	2.02
	et	4.810	-4.810	4.745	1.154	10.77	1.97
	DMF	4.809	-4.809	4.744	1.154	10.77	1.97
	DMSO	4.808	-4.808	4.744	1.154	10.77	1.97
	water	4.807	-4.807	4.743	1.154	10.77	1.97

B2 < A1 < A2 < B1 < A3. According to these results, it can be easily estimated that B2 and A3 structures have the largest ΔN max value in the gas phase and also in the solvent phase. Increase in the max charge transfer values of B2, A2, A1, B1, A3 in gas phase are 2.21 %, 3.09 %, 13.79 %, and 1.55 % (**Table 3**).

The Energy Gaps (ΔE) for the favipiravir form studied increase in the following order: A3 < B1 < A1 < A2 < B2 for gas phase and the other solvent phases at B3LYP/6311G(d, p). Also, the energy gap of favipiravir form has depended on the solvent media. The most significant difference of energy gap for water and gas phases is 0.05 eV, 0.12 eV, 0.13 eV respectively for A1, A2, and B2 forms, however, energy gap in water is smaller than gas phase only 0.01 eV for A3 and 0.04 for B1.

Dipol moment, which is a measurement of the asymmetry in the charge distribution, indicates the degree of separation of the charge in a molecule. The number of atoms in tautomers is constant, and it is stated that only the movement of the H atom between N and O atomic regions can bring important properties in tautomeric structures in which it is evaluated. The trends can be seen much better with the values of dipole moments (DM), where different values of the DM can detect different directions of the electronic directions. The dipole moments of Favipiravir's A1, A2, A3, B1, B2 forms and transition states (TS1, TS2, and TS3) between A1 and A2, A2 and A3 and B1 and A3 were calculated in the gas and solvent phases and are given in Fig. 3.

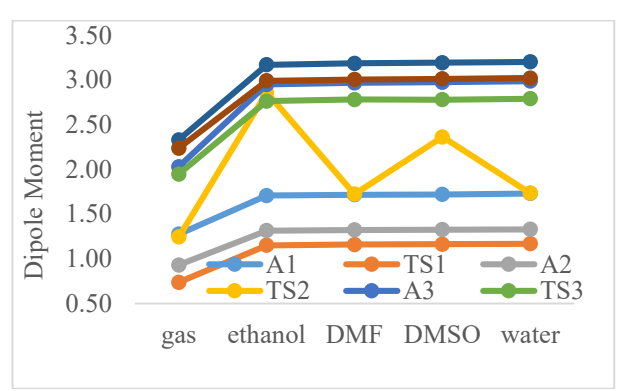


Fig. 3. The dipole moments μ (D) of A1, A2, A3, B1, B2 forms and transition states in different media.

The values of the dipole moments in Figure 4 show that the presence of the solvent generally increases in the dipole moment of the A1, A2, A3, B1, B2 form of favipiravir and transition states relative to the gas phase. The dipole moments increase by changing the gas phase to the solution as well as by increasing the solvent polarity. In more polar solvents, Polar solvents have higher dipole moment values than non-polar solvents, so delocalization of loads is higher in polar solvents [30-32]. The gaseous A1, A2, A3, B1 and B2 forms have a dipole moment value of 1.28, 0.93, 2.03, 2.33 and 2.24 D in the gas phase. A2 tautomer has smaller dipole moments than the other forms, and B1 form has an enormous dipole moment.

The polarity of organic materials is usually due to the contributions of the components of the system (atoms, molecules) due to the molecules' Van der Waals, dipole-dipole interactions, hydrogen bond interactions. The nonlinear optical properties of molecular systems depend on the polarization of electrons in their bonding orbitals. The mean polarization and anisotropy of the polarization (α a and $\Delta\alpha$) were calculated as follows using the polarization component

$$\alpha = \frac{1}{3} (\alpha_{xx} + \alpha_{yy} + \alpha_{zz})$$

$$\Delta \alpha = \left[\frac{(\alpha_{xx} - \alpha_{yy})^2 + (\alpha_{yy} - \alpha_{zz})^2 + (\alpha_{zz} - \alpha_{xx})^2 + 6(\alpha_{xz}^2 + \alpha_{xy}^2 + \alpha_{yz}^2)}{2} \right]^{1/2}$$

The results of the static polarizability of A1, A2, A3, B1, B2 forms and TS1, TS2 and TS3 transition states of favipiravir calculated in the gas phase and different solvents are shown in **Fig. 4.** The highest $<\alpha>$ value was found as 15.63 for A3 in water phases. Furthermore, the dipole moment difference between gas and water phase is the biggest; this difference is 3.53 esu, 3.48 esu, 3.76 esu, 3.75 esu, 3.46 esu, respectively for the forms A1, A2, A3, B1 and B2.

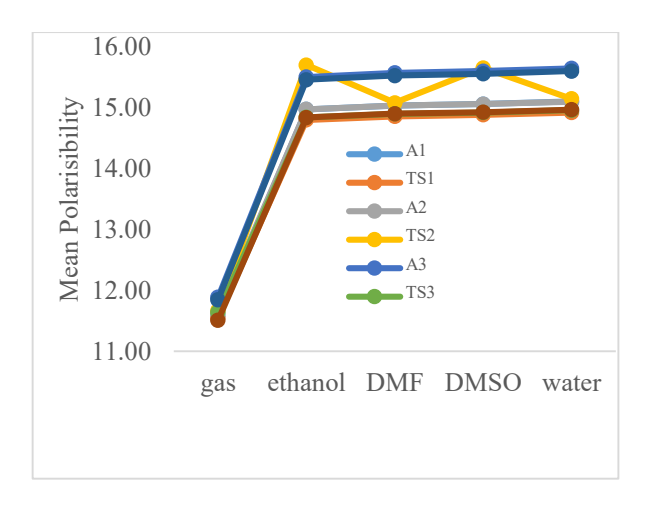


Fig. 4. The average polarizability α (esu) of A1, A2, A3, B1, B2 forms and transition states in different media

Static values of polarizability evolve in the following order B2<B1< in gas phase and different media, and static values of polarizability evolve in the following order A3<A2<A1 in gas phase, but A3<A2=A1.

The high polarity of a molecule means that the molecule has a small frontier orbital gap. [33-36] Form A3 has the smallest frontier orbital gap energy in the gas phase and the largest polarization of the favipiravir forms examined, so this is associated with a high chemical reactivity, low kinetic stability and is also termed as a soft molecule.

Frontier orbital gap energy of A3 form in the solvent phase is smaller than the gas phase so, it could be concluded that A3 form in the solvent phase is a higher chemical reactivity than the gas phase. **Fig. 4** shows that polar solvents increase the polarisability of all studied favipiravir tautomers in compare to the gas phase.

Results of polarization anisotropy calculated in the gas phase and different solvents of the forms of Favipiravir molecule A1, A2, A3, B1, B2 and their transition states are shown in **Fig. 5.**

For these forms, the anisotropy of polarizability is found as 9.95, 9.76, 10.18, 10.57, 9.78 in the gas phase, and as 13.42, 13.16, 14.31, 14.64, 13.17 in the water phase. The most significant difference in polarization anisotropy value was found between the water and gas phases, which are 3.48 esu, 3.39 esu, 4.14 esu, 4.07 esu, 3.39 esu for A1, A2, A3, B1 and B2 forms, respectively.

The total hyperpolarizabilities in atomic units (a.u.) are related to the electrostatic units (esu) by the relation: 1 a.u. = 8.6393X10-33 esu. The first hyperpolarizability is a third-degree tensor that can be defined by a 3 x 3 x 3 matrix. Due to the Kleinman symmetry, 27 components of the 3-D matrix can be reduced to 10 components. The output of Gaussian 09 provides ten components of this matrix as βxxx , βxxy , βxyy , βxyy , βxyz ,

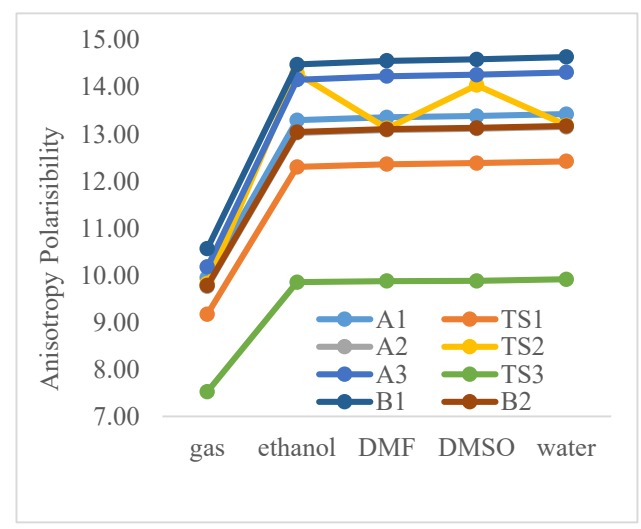


Fig. 5 Polarization anisotropy values calculated in the gas phase and different solvents of the forms of Favipiravir molecule A1, A2, A3, B1, B2 and their transition states

Thermodynamic parameters such as heat capacity $\binom{C_{p,m}^o}{p,m}$, entropy $\binom{S_{p,m}^o}{p,m}$ and enthalpy $\binom{H_{p,m}^o}{p,m}$, changes Gibbs Free energy changes $\binom{G_{p,m}^o}{p,m}$ were calculated for the A3 favipiravir form at temperatures ranging from 200 K to 1000 K, under 1 atm pressure and vacuum. Based on vibration analysis, these static thermodynamic functions were obtained from theoretical harmonic frequencies and their correlation graphs are shown in **Fig. 6**.

It can be observed from **Fig. 6** that heat capacity, entropy, and enthalpy of favipiravir increase with temperatures ranging from 200 to 1000 K due to increased molecular vibration intensities with temperature and Gibbs free energy of For A3 favipiravir form decreases. It means that with increase of temperature, the stability of A3 favipiravir

form increases [37]. Correlation equations between heat capacity, entropy, enthalpy, Gibbs Free energy changes and temperatures were placed by quadratic formulas as in the equation below with the corresponding fit factors (R^m) for these thermodynamic properties are 0.9983, 0.9999 and 0.9997, 1.000 respectively.

$$C_{p,m}^o = -6x10^{-5}T^2 + 0.1194T + 4.9341$$

 $S_{p,m}^o = -4x10^{-5}T^2 + 0.1491T - 56.726$
 $H_{p,m}^o = 2x10^{-5}T^2 + 0.0264T - 3.3117$
 $G_{p,m}^o = -5x10^{-5}T^2 + 0.0707T + 2.8816$

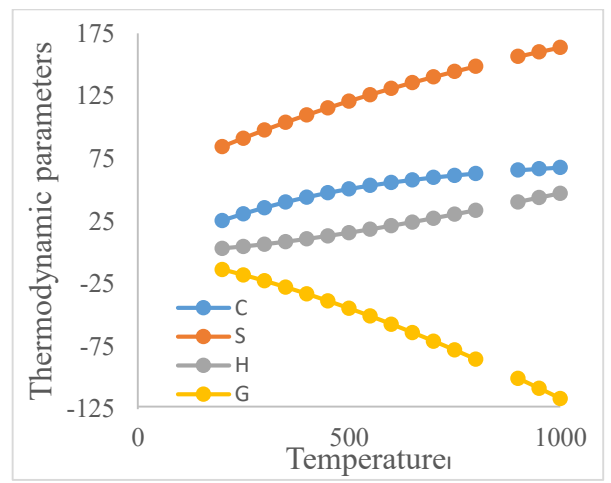


Fig. 6. Plots of the Heat capacity (Enthalpy H (in kcal mol⁻¹), Gibbs free energies G (in Kcal mol⁻¹) Entropy S (in kcal mol⁻¹), of versus temperature (K), of favipiravir

4. Conclusions

In this research, we have tried to explain quantum chemical parameters of the A1, A2, A3, B1, B2 form of favipiravir and transition states TS1 between A1 and A2 forms, TS2, A2 and A3 forms and TS3 A3 and B1 forms in gas and studied solvent phase at B3LYPP/6-311G(d, p) to show the computed parameters strongly depend on the solvent media. The dipole moments, polarisability of all forms are affected by the solvent. With the increase of the polarity of solvents, the dipole moments of all tautomers were increased.

References

- [1] Y. Furuta K.Takahashi, K. Shiraki, K. Sakamoto, D.F. Smee, DL. Barnard, et al., "T-705 (favipiravir) and related compounds: Novel broad-spectrum inhibitors of RNA viral infections", Antiviral Res, vol. 82(3), pp. 95-102. 2009
- [2] H. Sangawa, T. Komeno, H. Nishikawa, A. Yoshida, K. Takahashi, N. Nomura et al. Mechanism of action of T-705 ribosyl triphosphate against influenza virus RNA polymerase. Antimicrob Agents Chemother, vol. 57(11), pp. 5202-5208, 2013.

- [3] K. Yamada, K. Noguchi, T. Komeno, Y. Furuta, A. Nishizono, Efficacy of Favipiravir (T-705) in Rabies Postexposure Prophylaxis, J. Infect Dis., vol. 213(8), pp. 1253-1261, 2016.
- [4] L. Delang, N. Segura Guerrero, A. Tas, G. Quérat, B. Pastorino, et al. Mutations in the chikungunya virus non-structural proteins cause resistance to favipiravir (T-705), a broadspectrum antiviral, J. Antimicrob Chemother., vol. 69(10), pp. 2770-2784, 2014.
- [5] Y. Furuta, B.B Gowen, K. Takahashi, K. Shiraki, D.F Smee, D.L. Barnard, Favipiravir (T-705), a novel viral RNA polymerase inhibitör, Antiviral Res., vol. 100(2), pp. 446-454, 2013.
- [6] B.E. Dawes, B. Kalveram, T. Ikegami, T. Juelich, J.K. Smith, L. Zhang, et al., Favipiravir (T-705) protects against Nipah virus infection in the hamster model, Sci Rep. Vol. 15(8), pp. 1-11, 2018.
- [7] G. Li, E. De Clercq, , Therapeutic options for the 2019 novel coronavirus (2019-nCoV)Nat. Rev. Drug Discov., vol. 19(3), pp. 149-150, 2020.
- [8] BRIEF-Corrected-Zhejiang Hisun Pharma gets approval for clinical trial to test flu drug favipiravir for pneumonia caused by new coronavirus. Reuters Healthcare, February 16, 2020
- [9] C. Parlak, Ö. Alver, M. Şenyel, Computational study on favipiravir adsorption onto undoped and Si-doped C60 fullerenes, J. Theor. Comput. Chem., Vol. 16(2), 2017.
- [10] Ö. Alver, C. Parlak, Y. Umar, P. Ramasami, DFT/QTAIM analysis of favipiravir adsorption on pristine and silicon doped C20 fullerenes. Main Group Met. Chem., Vol. 42(1), pp. 143-149, 2019.
- [11] K. Harismah, M. Mirzaei Favipiravir: Structural Analysis and Activity against COVID-19. Adv. J. Chem. B., vol. 2(2), pp. 55-60, 2020
- [12] Q. Cai, M. Yang, D. Liu, J. Chen, D. Shu, Xia J et al. Experimental Treatment with Favipiravir for COVID-19: An Open-Label Control StudyEngineering, vol. 6(10), pp. 11092-11098, 2020.
- [13] H.S.Sayiner, A.A.S. Abdalrahm, M.A. Başaran, V. Kovalishyn, F. Kandemirli. The Quantum Chemical and QSAR Studies on Acinetobacter Baumannii Oxphos Inhibitors Med. Chem., vol. 14(3) pp. 253-268, 2018. 2007
- [14] T. Bakır, H.S. Sayiner, F. Kandemirli, Experimental and theoretical investigation of antioxidant activity and capacity of thiosemicarbazones based on isatin derivatives, Phosphorus, Sulfur Silicon Relat. Elem. Vol. 193(8), pp. 493-499,2018.
- [15] M.A. Ansari, S. Mohiuddin, F. Kandemirli, M.I. Malik. Synthesis and characterization of poly(3-

- hexylthiophene): improvement of regioregularity and energy band gap. RSC Adv. Vol. 8, pp. 8319-8328, 2018.
- [16] H.S. Sayiner, F. Genç, F. Kandemirli, Study of Interaction between Tigecycline and Sulbactam J. Pharm. Res. Int., vol. 26(1), pp. 1-9, 2019.
- [17] J. Frisch, M. Trucks, G.W.Schlegel, H.B. Scuseria, G.E. Robb, M.A. Cheeseman, Et al. Gaussian Inc, Wallingford CT 2009.
- [18] H.P. Hratchian, H.B. Schlegel, Accurate reaction paths using a Hessian based predictor–corrector integrator J. Chem. Phys. Vol. 120(21), pp. 9918-9924, 2004.
- [19] H.P Hratchian, H.B. Schlegel Using Hessian Updating To Increase the Efficiency of a Hessian Based Predictor-Corrector Reaction Path Following MethodJ. Chem. Theory Comput, vol. 1(1), pp. 61-69, 2006.
- [20] Y. Takano, K.N. Houk. Benchmarking the Conductor-like Polarizable Continuum Model (CPCM) for Aqueous Solvation Free Energies of Neutral and Ionic Organic Molecules. J. Chem. Theory Comput., vol. 1(1), pp. 70-77, 2005.
- [21] L. Onsager, Electric Moments of Molecules in Liquids J. Am. Chem. Soc., vol. 58(8), pp. 1486-1493, 1936
- [22] K. Fukui, Role of Frontier Orbitals in Chemical Reactions, Science Science, vol. 218, pp. 747-754, 1982.
- [23] P.W. Ayers, J.S.M, Anderson, L. Bartolotti, Perturbative perspectives on the chemical reaction prediction problem. J. Int. J. Quantum Chem. Vol. 101(5), 2005
- [24] T. Koopmans, Über die Zuordnung von Wellenfunktionen und Eigenwerten zu den Einzelnen Elektronen Eines AtomsPhysica1, vol. 6 pp. 104-113, 1933
- [25] R.G.Parr, R.G. Pearson, Absolute hardness: companion parameter to absolute electronegativity.

 J. Am. Chem. Soc., vol. 105(26), pp. 7512-7516, 1983
- [26] J. Padmanabhan, R. Parthasarathi, V. Subramaniaan, P.K. Chattaraj, Electrophilicity-Based Charge Transfer Descriptor J. Phys. Chem.,;vol. 111(7), pp. 1358-1361, 2007.
- [27] R.G. Pearson, Absolute electronegativity and hardness: applications to organic chemistryJ. Org. Chem., vol. 54(6), pp. 1424-1430, 1989.
- [28] R.G, Parr W. Yang Density functional approach to the frontier-electron theory of chemical reactivityJ. Am. Chem. Soc., vol. 106(14), pp. 4049-4050 1984.

- [29] P.K. Chattaraj, S. Giri, Stability, Reactivity, and Aromaticity of Compounds of a Multivalent SuperatomJ. Phys. Chem., vol. 111(43), pp. 11116-11121, 2007.
- [30] A. Ahmed. E/Z-Iminol Conformational behavior of the substituted formohydroxamic: A DFT study J. Chem. Pharm. Res. 7(4) (2015) 1215-1221
- [31] Š. Budzák, M. Medved, B. Mennucci, D.J Jacquemin, Unveiling Solvents Effect on Excited-State Polarizabilities with the Corrected Linear-Response ModelPhys. Chem. A., vol. 118(30), pp. 5652-5656, 2014.
- [32] M.T. Samani, S.M.Hashemianzadeh Study of solvent effect on thermodynamic stability and electron efficiency of MZ-341 dyeJ. Mol. Liq. Vol. 273, pp. 27-32, 2019.
- [33] L. Sinha, O. Prasad, V. Narayan, S.R. Shukla, Raman, FT-IR spectroscopic analysis and first-order hyperpolarisability of 3-benzoyl-5-chlorouracil by first principlesJ. Mol. Simul., vol. 37, pp. 153-63, 2011.
- [34] B. Kosar, C. Albayrak Spectroscopic investigations and quantum chemical computational study of (E)-4-methoxy-2-[(p-tolylimino)methyl]phenol, Spectrochim Acta. Vol. 78(1) pp. 160-167, 2011.
- [35] T. Abbaz, A Bendjeddou, D. Villemin, Molecular structure, HOMO, LUMO, MEP, natural bond orbital analysis of benzo and anthraquinodimethane derivativesPharm. biol. eval. 5(2) (2018) 27-39
- [36] D.F, Lewis, C. Ioannides, D.V. Parke, Interaction of a series of nitriles with the alcohol-inducible isoform of P450: Computer analysis of structureactivity relationships, Xenobiotica. Vol. 24(5) pp. 401-408, 1994.
- [37] J.B. Ott, J.B. Goates, Calculations from Statistical Thermodynamics, Academic Press, 2000